

Identification of Contaminating Particle Geometry in a Co-axial Configuration Using Trichel Pulse Characteristics

M. M. El Bahy¹, S. A. Ward², R. Morsi² and M. Badawi²

¹Faculty of Engineering at Benha, Benha University, Egypt

²Faculty of Engineering at Shoubra, Benha University, Egypt

Abstract- A method is presented for detecting and identifying the shape and size of a contaminating metallic particle in gas insulated system (GIS). A fixed particle-initiated negative corona in air insulated co-axial cylindrical configuration is investigated at a voltage slightly above the corona onset level. The characteristics of the negative corona pulses (Trichel pulses) are calculated by mathematical modeling the process taking place during the negative corona discharge. An experimental set-up is built up to measure the Trichel pulse characteristics and to check the accuracy of the present calculation. The calculated values of corona Trichel pulse amplitudes and repetition rates agree well with the measured values. So, the Trichel pulse characteristics are calculated for different particle sizes and shapes. These data of pulses are used as a bias for designing and training the artificial neural network technique (ANN). For earlier detection of insulation defect, the Trichel pulse characteristics are measured and then given as an input data to the trained ANN. Then, we could identify the particle shape and size.

I. INTRODUCTION

The gas insulated system (GIS) is widely used in electric power systems because of its compactness, maintenance free, safe and reliable operation. However, existence of a defect like particle or protrusion inside GIS affects its reliability and limit the equipment life time since the particle initiates partial discharge (PD) which may lead to complete failure of insulation structure [1-4]. Therefore, the detection of changes in insulation at early stages and the identification of particle geometry play an important role in increasing the service life time of the equipment [5].

Negative corona discharge starts with pulsating corona current, Trichel pulse, which is a train of regular pulse shape comprising sharp current peaks of short duration (ten of nanoseconds) separated by long inter-pulse period (ten of microseconds) [6]. The characteristics of the Trichel pulse, pulse amplitude, duration and repetition rate are affected by particle shape and size. So, these characteristics can be used as a tool in identification of particle geometry.

In this paper, the identification of contaminating conducting particle geometry in air insulated co-axial configuration is presented by utilizing the calculated and measured characteristics of particle-initiated Trichel pulse in a combination with ANN. The co-axial configuration is used for simulating the structure of GIS. The conducting particles are of spheres and wires of different sizes fixed on inner cylinder.

The wire particle is a cylinder hemispherically terminated at both ends positioned to touch radially the inner cylinder [4].

The calculated characteristics of Trichel pulse is based on mathematical modeling the process taking place during negative corona discharge [7]. As these processes are field dependent, the charge simulation technique is used for calculating the electric field in the vicinity of particle tip. The measured characteristics are obtained through an experimental high voltage test with a voltage magnitude slightly above onset voltage level. The calculated characteristics of Trichel pulse agreed well with the measured values and this agreement enable us to take the calculated pulse characteristics for different particles sizes for training ANN. The trained neural network is then used in the identification of any particle geometry by using its corresponding Trichel pulse characteristics, obtained experimentally, as an input data.

II. EXPERIMENTAL SET-UP

The experimental set-up is schematically illustrated in Fig. 1, this set-up has been built up to measure the characteristics of negative corona current pulse initiated by a particle fixed on the inner cylinder of air insulated co-axial configuration. The experimental work was carried out inside laboratory in dry air at room temperature (22-25°C) and atmospheric pressure using co-axial cylindrical configuration made of brass. The co-axial configurations had inner and outer cylinders of radii 5.5 and 41 mm, respectively. The inner cylinder length is 800 mm supported at both ends by insulating supports and is extended along the axis of 200 mm long outer cylinder. The outer cylinder edge is smoothed and rounded to avoid flashover or early discharge, Fig. 1.

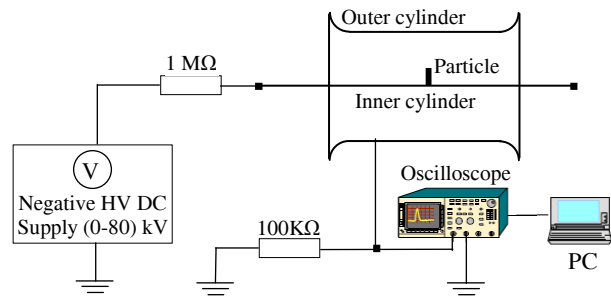


Fig. 1. Schematic diagram of experimental set-up.

Spherical and wire particle of different dimensions were used in experiment and each particle is fixed on the inner cylinder. Stainless steel spherical particles of radii 1.6 and 2.4 mm were used. Also, tin wire particles of radii 0.375 and 0.5 mm with varying lengths in the range 3 to 15 mm were used.

A high-voltage DC source with negative polarity and output voltage up to 80kV (Hipotronics, Model 880PL-10 mA) was used to energize the stressed cylinder. The high voltage source has a voltage metering device, for measuring the output applied voltage, with full scale accuracy of $\pm 2\%$. The stressed cylinder was connected to the HV source through a water resistance of $1M\Omega$ as a current limiting resistor, to prevent any damage of instruments if flashover occurred, and the other cylinder was grounded through $100k\Omega$ resistor. Digital storage oscilloscope (Gwinstek, Model GDS-1052-U), connected to the computer, was connected across $100k\Omega$ resistor to detect and monitor the negative corona current pulse. The detected corona current pulses have been recorded and saved to the computer.

III. METHOD OF ANALYSIS

A. Trichel Pulse Calculation

As well known, Trichel pulse calculation in the gap is field dependent [7-8]. Hence, for calculating the three dimensional field problem in the vicinity of a particle tip in a co-axial configuration, the charge simulation technique (CST) is used [4]. The corona current pulse (Trichel pulse) is a train of regular shape that appears in the external circuit when the H.V. electrode is stressed negatively above corona onset level. It corresponds to the rapid motion of electrons and ions generated from a number of primary avalanches growing simultaneously at various points on the particle tip, inside the ionization zone. Each one of these avalanches is accompanied by a series of auxiliary successive avalanches during its life [7-8]. With the formation of primary avalanche and its auxiliary, more positive ions are accumulated and the ionization zone boundary is narrowed. Hence, the auxiliary avalanche current is decreased until stopping the ionization process and eventually no more avalanche are produced. Then, the current in the gap vanishes. After the removal of space charges from the discharge zone, a new current pulse appears in the circuit [7-8].

1) *The Contribution of Primary Avalanches to Trichel Pulse:* Inside the ionization zone, the current pulse is initiated by a group of primary avalanches growing simultaneously at various points over the particle surface. During the travel of each primary avalanche away from the particle surface, it causes ionization by collision and photoionization of some gas molecules and some electrons get attached to gas molecules forming negative ions [4]. The number of electrons and the corresponding number of negative ions for each one of these avalanches, at a distance ξ from the starting point at the particle surface are [8-10]:

$$N_e(\xi) = e^{\int_0^{\xi} (\alpha - \eta) d\xi} \quad (1)$$

$$N_-(\xi) = \int_0^{\xi} \eta N_e(\xi) d\xi \quad (2)$$

where, α is the Townsend's first ionization coefficient and η is the electron attachment coefficient [4]. The growth calculation of any primary avalanche takes place under the resultant field produced by the applied field and that produced by the positive ion space charges developed within all preceding steps in the avalanche wake [7-9, 11-12].

The primary avalanche continues to grow in the ionization zone as long as $\alpha > \eta$. Reaching the ionization zone boundary (ξ_c), the electron avalanche ceases to grow. Surpassing this boundary, this number of electrons begins to get attached to neutral molecules forming negative ions, as in (3). However the life of avalanche continues outside the ionization zone until the boundary of corona layer (ξ_e), where 99.9% of the electrons in the avalanche get attached to air molecules forming negative ions, as in (4).

$$N_e(\xi) = N_e(\xi_c) e^{\int_{\xi_c}^{\xi} (-\eta) d\xi} \quad (3)$$

$$N_-(\xi) = \int_{\xi_c}^{\xi} \eta N_e(\xi) d\xi \quad (4)$$

The primary avalanches transit time at distance (ξ), is:

$$t(\xi) = \int_0^{\xi} (1/v_e) d\xi$$

The corresponding instantaneous value of the corona current for this avalanche is [7-8]:

$$i(\xi, t) = \frac{e \cdot N_e(\xi) \cdot v_e(\xi) E_r(\xi)}{V} \quad (5)$$

where, E_r is the resultant field produced by applied field and space charges field of the avalanche, v_e is the electron drift velocity [11] and V is the applied voltage. The number and the locations of primary avalanches, initiated at various points on particle surface, are determined as follows:

In Fig. (2-a), the simultaneous and parallel development of primary avalanches at particle tip is shown. One of the primary avalanches is developed at the maximum field line of particle tip ($\theta_i=0$) and the other number of primary avalanches are developed in layers involving each other. When the primary avalanche at maximum field line ($\theta_i=0, i=1$), reaches the ionization zone boundary, it has an apex angle:

$$d\theta_i = 2 \sin^{-1} \left[\frac{\sqrt{6D_e t(\mathcal{R}_i)}}{\mathcal{R}_i} \right]$$

where D_e is the electron diffusion coefficient and $t(\mathcal{R}_i)$ is the time elapsed to reach the ionization zone boundary. For a layer number i , it initiated at an angle $\theta_i = \sum_1^{i-1} d\theta_i$, distributed over

the surface around the z-axis. The number of primary avalanches in a layer i , $N(\theta_i)$, Fig. (3-b), is determined by dividing the circumference of the center line connecting all heads of the avalanches in this layer $\equiv (2\pi \mathcal{R}_i \sin \theta_i)$ by the diameter of one electron avalanche head $\equiv 2\sqrt{6D_e t(\mathcal{R}_i)}$ of the same layer.

The corona current of avalanches developed in each subsequent layer is added till the current value of a new layer is negligible i.e. $\leq 1\%$ of total corona current.

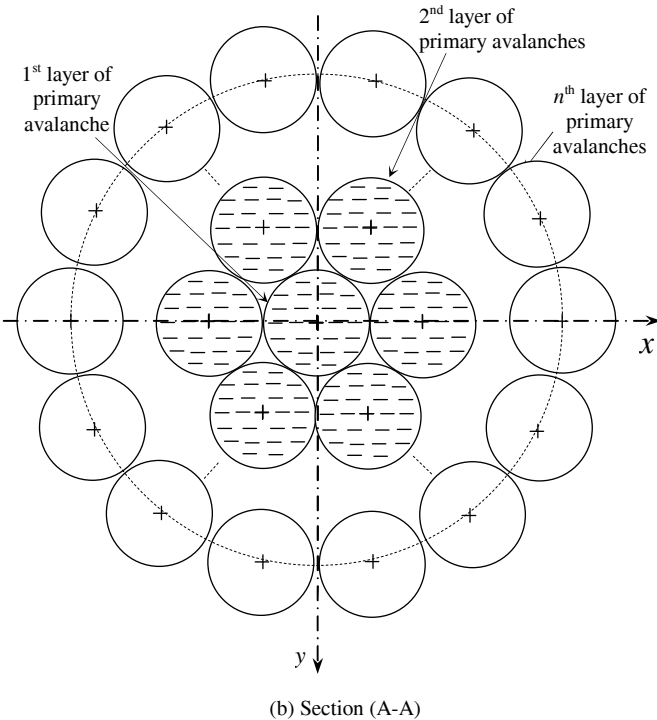
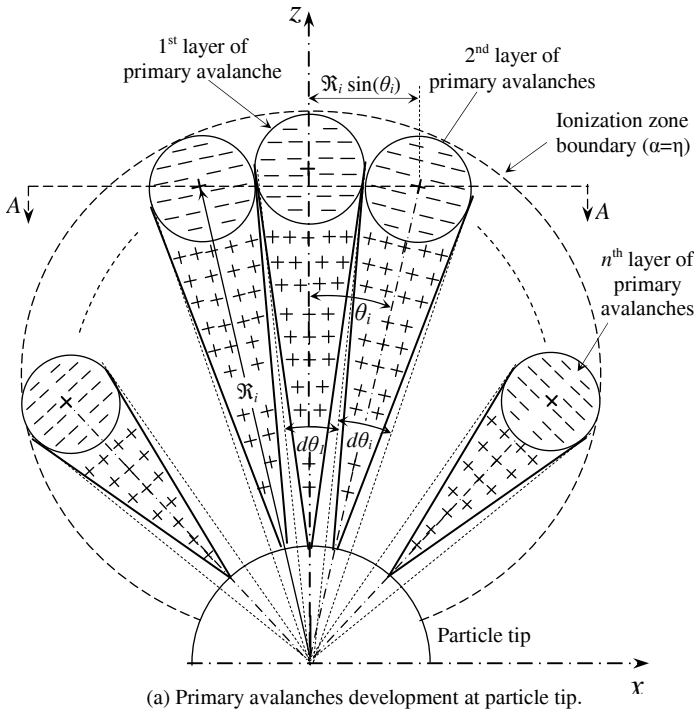


Fig 2. Primary avalanches development at particle tip in the ionization zone.

2) *The Contribution of Auxiliary Avalanches to Trichel pulse:* Along the path and the wake of each primary avalanche, a successor avalanche can be started when the preceding primary avalanche somehow provides an initiating electron at particle

surface, possible by photo-emission, positive ion impact, metastable or field emission. Only the first mechanism (electron emission from the cathode by photons) is the most efficient process in initiating a new auxiliary avalanche [4]. The number of photoelectrons emitted from particle surface, while the primary avalanche has travelled a distance ζ , is:

$$N_{eph} = \int_0^{\zeta} \gamma_p \cdot \alpha(\xi) \cdot Ne(\xi) \cdot g(\xi) \cdot e^{-\mu\xi} d\xi \quad (6)$$

where γ_{ph} is Townsend's second coefficient due to the action of photons, μ is the absorption coefficient in air and $g(\xi)$ is a geometric factor to account for the fact that some photons are not received by the cathode [4]. The first auxiliary avalanche gets launched at particle tip, when N_{eph} of primary avalanche reaches unity. Simultaneously with the growth of each primary avalanche, the auxiliary avalanche grows in the channel and along the wake of the primary avalanche. The growth of the auxiliary avalanche takes place under the resultant field composed of its own self-space charge field and the applied field distorted by space charges at all preceding steps left by the preceding avalanches.

During the growth of primary and auxiliary avalanches, the emitted photons from their avalanche heads contributes to the irradiation of the cathode surface leading to the emission of more and more photoelectrons which start new avalanches and so on. The total pulse current corresponds to the sum of the currents of primary and its auxiliary avalanches, each added up ordinate by ordinate in its respective time of production.

3) *Choking of electron Avalanches:* Due to the formation of primary avalanche and all its accompanied auxiliary avalanches, the discharge layer is fully complete with space charges, a positive cloud is formed near particle surface inside ionization zone and a cloud of negative ions is formed far from the particle surface outside ionization zone [7]. The positive ions assist the field near the particle and oppose it at point between the positive and negative ions. With more avalanches and accumulation of more positive ions, the ionization zone boundary is narrowed; the auxiliary avalanche current is decreased, the ionization process stops and eventually no more avalanches are produced.

(4) *Initiation of Subsequent Pulse:* Since the accumulation of positive ions near particle surface is the main cause of narrowing ionization zone, stopping the ionization process and damping the avalanche growth, so, the subsequent pulse cannot be initiated until the removal of space charges left in the discharge zone (ζ_e). The positive ions swept to the high voltage conductor, where they get neutralized and the negative ions move so far from the conductor until their residual field strength at corona layer boundary becomes negligible. i.e., 0.1% to 1% of the applied field strength (at $\zeta = \zeta_e$) [7]. The time required to remove all negative ions from corona layer is:

$$t_{r-} = \int_0^{\zeta_e} \frac{d\xi}{\mu \cdot E_r}$$

where, μ_- is mobility of negative ions [10], and E_r is the resultant field produced by applied field, the positive ion space charges produced at all preceding steps in ionization zone and the negative ions space charges at all preceding steps.

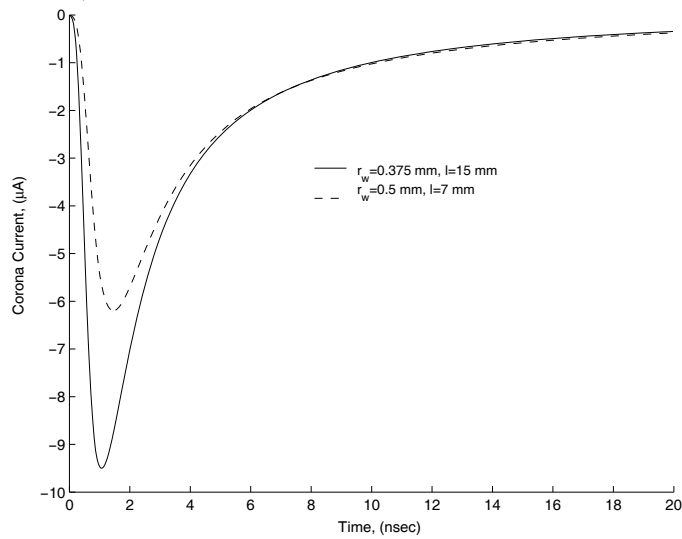
B. Neural Network Design:

An artificial neural network-based inference engine is devised, which enables the examiner to gain knowledge of the contaminating particle geometry based on the calculated characteristics of Trichel pulse initiated by a particle fixed at the inner cylinder of a co-axial configuration [13]. The calculated characteristics, pulse peak current and repetition rate as well as the corresponding applied voltage for different particle dimensions are used as training parameters for the feed-forward back propagation neural network in Matlab. The network is trained to provide us with the particle length and radius for other Trichel pulse characteristics obtained experimentally.

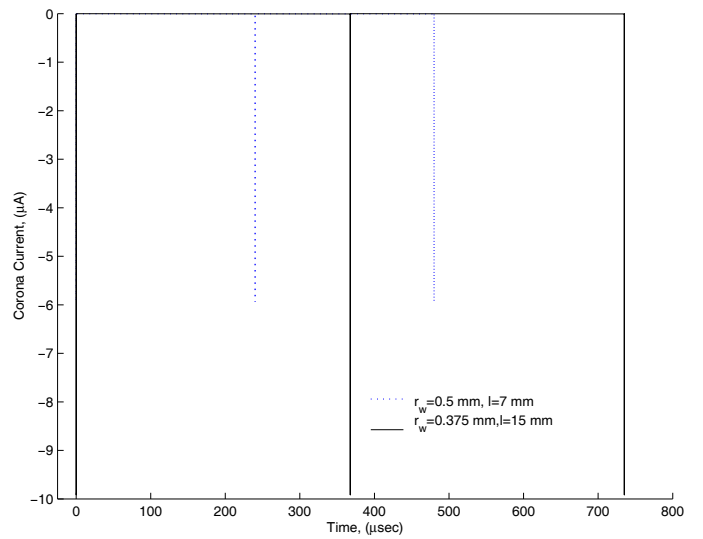
IV. RESULTS AND DISCUSSIONS

A. The Calculated Trichel Pulse Characteristics

The characteristics of the Trichel pulse initiated by a particle fixed on the inner cylinder of co-axial configuration ($r=5.5\text{mm}$, $R=41\text{mm}$) have been calculated at an applied voltage slightly above onset level (1.05% of the negative corona onset voltage) to get regular pulses since the current pulse at onset level is irregular pulses [14]. Fig. (3-a), shows the waveform of one negative corona current pulse initiated by wire particles of different radii, fixed on the inner cylinder. This pulse shows the calculated peak current, rise and decay time of the current pulse. The rise time is extremely short, on the order of 10^{-9} sec as obtained before [14]. Fig. (3-b), shows a train of the negative corona current pulses initiated by the same wire particles. This figure shows the calculated frequency of the current pulse. The corona current contribution of avalanches in outer layers surrounding the primary avalanches at maximum field line are added to the total corona current until the layer at which its current contribution is negligible (1% of total corona current).



(a) The waveform of one negative corona current pulse



(b) The train of negative corona current pulses

Fig. 3. The Trichel pulse waveform initiated by wire particles.

Fig. 4, shows the waveform of one negative corona current pulse initiated by spherical particles of different radii, ($r_s=1.6\text{mm}$ and 2.4mm), fixed on the inner cylinder. This pulse shows the calculated peak current, rise and decay time of the current pulse.

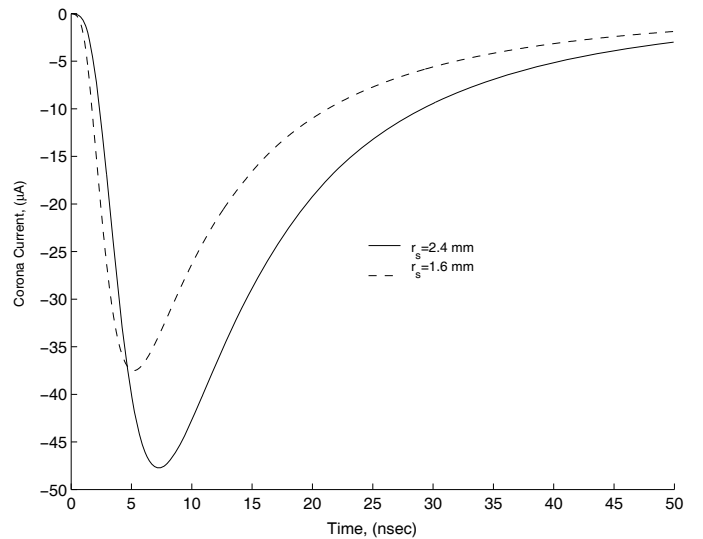


Fig. 4. The Trichel pulse waveform initiated by spherical particles.

B. The Measured Trichel Pulse Characteristics:

Laboratory measurements of the characteristics of Trichel pulse initiated by a particle fixed on the inner cylinder of a co-axial configuration were carried out to check the accuracy of the present calculation, and to be used as an input data to the trained ANN for obtaining the corresponding particle shape and size. The calculated values were corrected to the ambient temperature and pressure [4]. Fig. 5 and 6, shows the measured Trichel pulse waveforms initiated by wire particle ($r_w=0.5\text{mm}$ and $l=7\text{mm}$) and ($r_w=0.375\text{mm}$ and $l=15\text{mm}$) respectively, fixed on the inner cylinder.

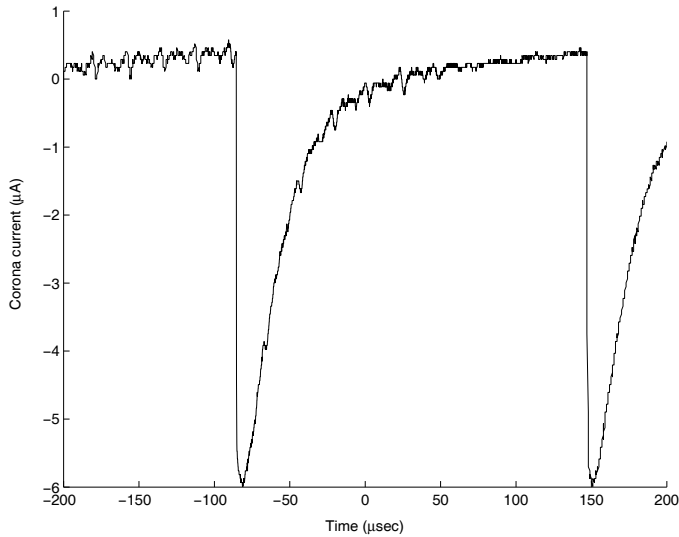


Fig. 5. The Trichel pulse waveform initiated by wire particle ($r_w=0.5$, $l=7$ mm).

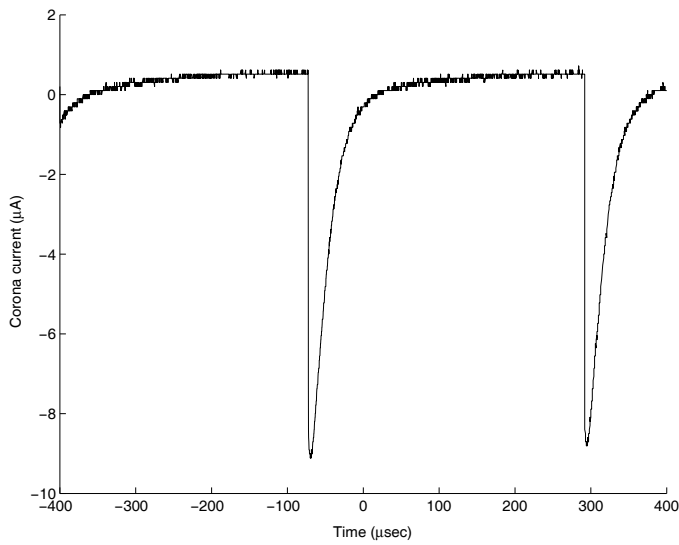


Fig. 6. The Trichel pulse waveform initiated by wire particle ($r_w=0.375$, $l=15$ mm).

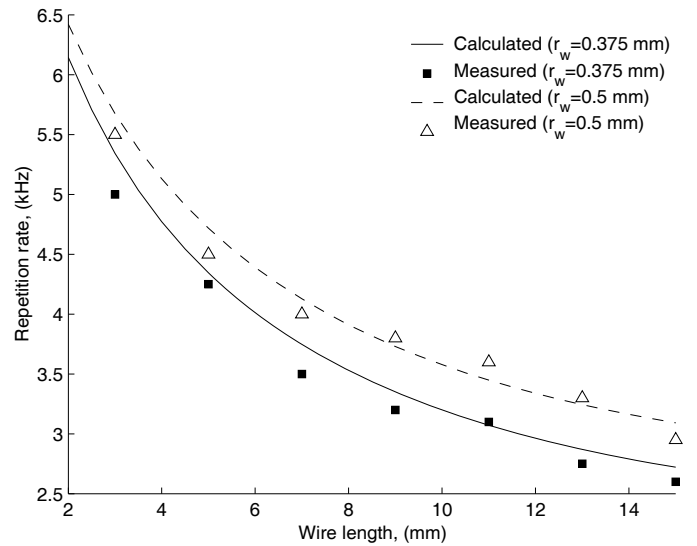


Fig. 7. Variation of Trichel pulse frequency initiated by wire particle, of different radii.

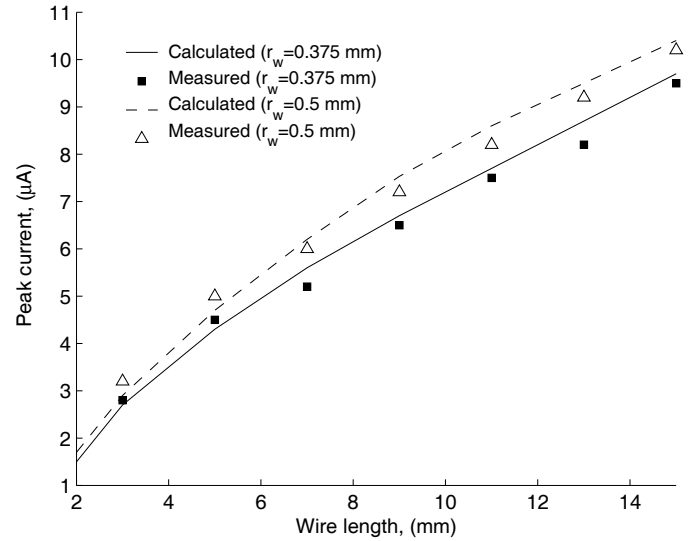


Fig. 8. Variation of the Trichel pulse peak current initiated by wire particle, of different radii.

C. Comparison Between Calculated and Measured Pulse Characteristics

Figures 7 and 8 shows the calculated and measured characteristics, pulse frequency and peak current, of the Trichel pulse initiated by wire particle of different radii fixed on the inner cylinder. The characteristics are obtained at an applied voltage slightly above onset level (1.05%) to get regular pulses since the current pulse at onset level is irregular pulses [14]. The characteristics of Trichel pulse varies with the particle shape and size. The calculated values agree well with those measured experimentally which prove the accurate of the mathematical modelling of Trichel pulse. For a wire particle, The Trichel pulse peak current increases with increasing particle length and its radius, while, the Trichel pulse frequency increases with decreasing particle length and increasing its radius.

TABLE 1
THE CALCULATED AND MEASURED CHARACTERISTICS OF TRICHEL PULSE INITIATED BY SPHERICAL PARTICLE

r_s (mm)	Applied Voltage (kV)	Calculated characteristics		Measured characteristics	
		Peak Current (uA)	Frequency (kHz)	Peak current (uA)	Frequency (kHz)
1.6	25.23	37.5	5.41	35	5.4
2.4	26.12	47.8	5.385	45	5.1

For a spherical particle, with increasing radius of spherical particle, the Trichel pulse peak current increases and the pulse repetition rate decreases.

D. Particle identification

The calculated characteristics of Trichel pulse, pulse peak current, repetition rate as well as the applied voltage for wire particles of radii 0.25, 0.375 and 0.5 with lengths 1.5 to 15.5 mm and spherical particles with radii 0.5 to 2.9 mm are used as training parameters for ANN using neural tool box in Matlab. The characteristics of other particles, obtained experimentally are fed to the trained ANN to obtain the predicted values of particle dimensions, and these particle dimensions are in Table 2.

TABLE 2
THE DIMENSIONS OF PARTICLES FED TO THE TRAINED ANN

Particle geometry	Radius (mm)	Length (mm)
Sphere	1.6-2.4	3.2-4.8
Wire	0.375	5-7-9-11-13
	0.5	5-7-9-11-13

The calculated characteristics input to ANN along with the corresponding predicted particle dimensions and the calculated percent error for each case are shown in Table 3. The error in the output values does not exceed 5.3% [13].

TABLE 3
INPUTS AND OUTPUTS OF THE TRAINED ANN (ERROR GOAL=0.0001)

Applied Voltage (kV)	Peak Current (uA)	Repetition Rate (kHz)	Particle shape	Radius (mm)	% error	Length (mm)	% error
25.23	35	5.4	sphere	1.598	-0.14	3.20	0.028
26.11	45	5.1	sphere	2.399	-0.29	4.80	0.05
11.87	4.5	4.25	wire	0.37	-0.21	5.00	0.026
10.14	5.2	3.5	wire	0.395	5.3	6.926	-1.06
9.07	6.5	3.2	wire	0.394	5.06	8.812	2.08
8.3	7.5	3.1	wire	0.375	0.053	11.22	2.03
7.75	8.2	2.75	wire	0.371	-1.01	12.93	-0.54
13.4	5	4.5	wire	0.499	-0.06	5.001	0.04
11.55	6	4	wire	0.500	0	7.002	0.04
10.38	7.1	3.8	wire	0.507	1.3	9.186	2.06
9.55	8	3.6	wire	0.495	-1.06	10.97	-0.22
8.93	9.1	3.3	wire	0.494	-1.3	12.9	-0.75

V. CONCLUSIONS

- The characteristics of particle-initiated corona Trichel pulse have been calculated based on mathematical modeling the process taking place during negative corona discharge.
- The calculated values of Trichel pulse characteristics agreed well with the values measured experimentally.
- For a wire particle, the Trichel pulse peak current increases with increasing length and radius, while, the Trichel pulse frequency increases with decreasing length and increasing radius.

- For a spherical particle, with increasing radius of spherical particle, the Trichel pulse peak current increases and the pulse repetition rate decreases.
- The particle shape and size are well identified using the experimental characteristics of negative corona current pulse as an input data to ANN.
- The particle dimensions are revealed after a very short time using the designed ANN with accuracy within 5.3%.

ACKNOWLEDGMENT

The authors are indebted to Professor Mazen Abdel-Salam, Assuit University, Egypt for his helpful suggestions.

REFERENCES

- [1] Kanako Nishizawa, Takashi Okusu, Hiroki Kojima, Naoki Hayakawa, Fumihiro Endo, Masanobu Yoshida, Katsumi Uchida, and Hitoshi Okub, "Particle size identification in GIS by ultra-high speed measurement of partial discharge", International Conference on Condition Monitoring and Diagnosis, 2008.
- [2] F. Endo, H. Okubo, K. Nishizawa, N. Hayakawa, M. Yoshida, T. Ogawa and H. Okuba, "High speed measurement and analysis of partial discharge pulses in SF6 gas insulated system", XVth International Symposium on High Voltage Engineering, ISH 2007, pp. 1-5.
- [3] H. Kojima, N. Hayakawa, F. Endo and H. Okubo, "Novel measurement and analysis system for investigation of partial discharge mechanism in SF6 gas", 12th International Middle-East Power System Conference, MEPCON 2008, pp. 75-79.
- [4] M. M. El-Bahy, S. A. Ward, R. Morsi and M. Badawi, "Onset voltage of a particle initiated negative corona in a co-axial cylindrical configuration" Journal of Physics D: Applied Physics, vol. 46, pp. 1-10, 2013.
- [5] I. A. Metwally, "Status review on partial discharge measurement techniques in gas-insulated switchgear/lines" Journal of Electric Power System Research, vol. 69, pp. 25-36, 2004.
- [6] Paria Sattari, G. S. Peter Castle and Kazimierz Adamiak, "Numerical simulation of Trichel Pulses in a negative corona discharge in Air", IEEE Trans. on Industrial Applications, vol. 47, no. 4, pp. 1935-1943, 2011.
- [7] M. Khalifa and M. Abdel-Salam, "Improved Calculation of corona pulse characteristics", IEEE PES Winter Meeting, pp. 1693-1699, Jan/Feb. 1974.
- [8] M. Abdel-Salam, "Relation between corona and wind", Ph.D Thesis, University of Cairo, Giza, Egypt, 1973.
- [9] S. El-Debeiky and M. Khalifa, "Calculating the corona pulse characteristics and its radio interference", IEEE Trans. on PAS vol. PAS-90, no. 1, pp. 165-179, Jan/Feb. 1971.
- [10] M. Khalifa and S. El-Debeiky, "Analysis of the effect of humidity on DC corona power losses", Proc. IEE, vol. 118, no. 5, pp. 714-718, Mar. 1971.
- [11] H. Parekh and K. D. Srivastava "Effect of avalanche space charge field on the calculation of corona onset voltage", IEEE Trans. on Electrical Insulation, vol. EI-14, no. 4, pp. 181-192.
- [12] Yacine Bourek, Leila Makhnache, Nacereddine Nait Said and Rafik Kattan, "Determination of ionization condition characterizing the breakdown threshold of a point-plane air interval using fuzzy logic", Journal of Electric Power System Research, vol. 81, pp. 2038-2047, 2011.
- [13] R.M Sharkawy and H. Anis, "Acoustic-based particle detection in oil using artificial neural networks", IEEE Porto Power Tech Conference, 2001.
- [14] W. L. Lama and C. F. Gallo, "Systematic study of the electrical characteristics of the Trichel current pulses from negative needle-to-plane coronas", Journal of Physics D: Applied Physics, vol. 45, no. 1, pp. 103-113, 1974.